http://cneoformans.mlst.net and http://mlst.mycology lab.org are used for this study and the study of Mihara et al., respectively. To compare STs in this study with the large-scale investigation by Simwami et al. (14), we adopted the former database. A Chinese epidemiological study has shown that the majority of *C. neoformans* isolates exhibited the same ST, in which the nucleotide sequences of 5 loci examined (*GPD1*, IGS1, *LAC1*, *PLB1*, and *SOD1*) are identical to those of ST46 (19). Similarly, the nucleotide sequences of all 7 loci in the major ST of clinical isolates in Korea are the same as those of ST46 in this study (20). Together, ST46, a predominant ST in Japan (determined in this study), has so far been isolated in Thailand, China, Korea, and Japan, which are geographically close to each other, suggesting that ST46 isolates from Asia may have the same origin.

Seven strains from the facility G in the Kyushu region (NIIDCr0034–0040) were isolated within a year (2008–2009). Usually, this facility only diagnoses 1 or 2 cases of cryptococcosis per year. Therefore, the high frequency of cryptococcosis could indicate a possibility of outbreaks occurring in the vicinity of the facility G. MLST analysis of these 7 isolates in this study revealed that 6 isolates belong to ST46. The cases at the facility E in the Kanto region showed similar patterns: 7 strains (NIIDCr0024–0027 and 0030–0032) were isolated in 1 year (2010–2011) and 6 isolates exhibited ST46. Local molecular epidemiology restricted to a small area should be able to indicate that these 2 cases were potential outbreaks; however, using our cryptococcal MLST database, the ST46 strain can be recognized as the predominant strain type that is widespread in Japan. Therefore, the present MLST analysis seems less useful for predicting or tracing the infection route or infection source of cryptococcosis outbreaks in Japan. To investigate the actual origin of these outbreaks, novel epidemiological tools such as multilocus microsatellite typing and whole genome sequencing will be required.

In conclusion, we analyzed clinical isolates of *C. neoformans* obtained from multiple locations widely distributed in Japan by MLST, a molecular epidemiological method. Most clinical isolates belong to the same ST (ST46), and there is little geographic bias among the areas studied. This database will be useful for public health officials in designing and prioritizing efforts to prevent, diagnose, and treat cryptococcal disease.

Conflict of interest None to declare.

REFERENCES

1. Park, B.J., Wannemuehler, K.A., Marston, B.J., et al. (2009): Estimation of the current global burden of cryptococcal meningitis among persons living with HIV/AIDS. AIDS, 23, 525–530.
2. Franzot, S.P., Salkin, I.F. and Casadevall, A. (1999): *Cryptococcus neoformans* var. *grubii*: separate varietal status for *Cryptococcus neoformans* serotype A isolates. J. Clin. Microbiol., 37, 838–840.
3. Lengeler, K.B., Cox, G.M. and Heitman, J. (2001): Serotype AD strains of *Cryptococcus neoformans* are diploid or aneuploid and are heterozygous at the mating-type locus. Infect. Immun., 69, 115–122.
4. Xu, J., Luo, G., Vilgalys, R.J., et al. (2002): Multiple origins of hybrid strains of *Cryptococcus neoformans* with serotype AD. Microbiology, 148, 203–212.
5. Heitman, J., Kozel, T.R., Kwon-Chung, K.J., et al. (2010): *Cryptococcus* from Human Pathogen to Model Yeast. ASM Press, Washington, D.C.
6. Kwon-Chung, K.J. and Bennett, J.E. (1978): Distribution of α and a mating types of *Cryptococcus neoformans* among natural and clinical isolates. Am. J. Epidemiol., 108, 337–340.
7. Fraser, J.A., Giles, S.S., Wenink, E.C., et al. (2005): Same-sex mating and the origin of the Vancouver Island *Cryptococcus gattii* outbreak. Nature, 437, 1360–1364.
8. Lin, X., Litvintseva, A.P., Nielsen, K., et al. (2007): αADα hybrids of *Cryptococcus neoformans*: evidence of same-sex mating in nature and hybrid fitness. PLoS Genet., 3, 1975–1990.
9. Meyer, W., Castañeda, A., Jackson, S., et al. (2003): Molecular typing of IberoAmerican *Cryptococcus neoformans* isolates. Emerg. Infect. Dis., 9, 189–195.
10. Meyer, W., Aanensen, D.M., Boekhout, T., et al. (2009): Consensus multi-locus sequence typing scheme for *Cryptococcus neoformans* and *Cryptococcus gattii*. Med. Mycol., 47, 561–570.
11. Bovers, M., Hagen, F., Kuramae, E.E., et al. (2008): Six monophyletic lineages identified within *Cryptococcus neoformans* and *Cryptococcus gattii* by multi-locus sequence typing. Fungal Genet. Biol., 45, 400–421.
12. Ngamskulrungroj, P., Gilgado, F., Faganello, J., et al. (2009): Genetic diversity of the *Cryptococcus* species complex suggests that *Cryptococcus gattii* deserves to have varieties. PLoS ONE, 4, e5862.
13. Litvintseva, A.P., Thakur, R., Vilgalys, R., et al. (2006): Multilocus sequence typing reveals three genetic subpopulations of *Cryptococcus neoformans* var. *grubii* (serotype A), including a unique population in Botswana. Genetics, 172, 2223–2238.
14. Simwami, S.P., Khayhan, K., Henk, D.A., et al. (2011): Low diversity *Cryptococcus neoformans* variety *grubii* multilocus sequence types from Thailand are consistent with an ancestral African origin. PLoS Pathog., 7, e1001343.
15. Mihara, T., Izumikawa, K., Kakeya, H., et al. (2012): Multilocus sequence typing of *Cryptococcus neoformans* in non-HIV associated cryptococcosis in Nagasaki, Japan. Med. Mycol. Doi: 10.3109/13693786.2012.708883.
16. Barreto de Oliveira, M.T., Boekhout, T., Theelen, B., et al. (2004): *Cryptococcus neoformans* shows a remarkable genotypic diversity in Brazil. J. Clin. Microbiol., 42, 1356–1359.
17. Tamura, K. and Nei, M. (1993): Estimation of the number of nucleotide substitutions in the control region of mitochondrial DNA in humans and chimpanzees. Mol. Biol. Evol., 10, 512–526.
18. Tamura, K., Peterson, D., Peterson, N., et al. (2011): MEGA5: molecular evolutionary genetics analysis using maximum likelihood, evolutionary distance, and maximum parsimony methods. Mol. Biol. Evol., 28, 2731–2739.
19. Chen, J., Varma, A., Diaz, M.R., et al. (2008): *Cryptococcus neoformans* strains and infection in apparently immunocompetent patients, China. Emerg. Infect. Dis., 14, 755–762.
20. Choi, Y.H., Ngamskulrungroj, P., Varma, A., et al. (2010): Prevalence of the VNIc genotype of *Cryptococcus neoformans* in non-HIV-associated cryptococcosis in the Republic of Korea. FEMS Yeast Res., 10, 769–778.
21. Yasuoka, A., Kohno, S., Yamada, H., et al. (1994): Influence of molecular sizes of *Cryptococcus neoformans* capsular polysaccharide on phagocytosis. Microbiol. Immunol., 38, 851–856.

ORIGINAL ARTICLE

Impaired capsular polysaccharide is relevant to enhanced biofilm formation and lower virulence in *Streptococcus pneumoniae*

Liang Qin · Yutaka Kida · Yoshihiro Imamura · Koichi Kuwano · Hiroshi Watanabe

Abstract *Streptococcus pneumoniae* has been reported to form biofilms. Many different surface molecules, including capsular polysaccharide (CPS), may play a fundamental role in pneumococcal biofilm development. We designed a CPS mutant, TIGR4cps4D⁻, from the TIGR4 strain and detected enhanced biofilm formation. The pathogenic diversities of the mutant were also investigated with the in vitro expression levels of *pavA*, *lytA*, *IgA1*, *piaA*, *psaA*, *ply*, and *spxB*. The mean OD_{595} of TIGR4cps4D⁻ biofilm was 1.77 and 1.74, whereas that of TIGR4 was 0.76 and 0.33 on day 1 and day 2, respectively. Scanning electron microscopy and confocal laser scanning microscopy showed TIGR4cps4D⁻ formed a biofilm that was significantly thicker than that formed by TIGR4 ($\sim$12.22 vs. $\sim$6.29 μm). Compared to TIGR4, the gene expression of *lytA*, *IgA1*, and, *psaA* in TIGR4cps4D⁻ was 1.9×10^{-5}-, 2.4×10^{-5}-, and 3.2×10^{-3} fold lower under the planktonic condition, and 1.9×10^{-5}- and 9.7×10^{-5} fold lower in biofilms, respectively. Furthermore, TIGR4cps4D⁻ seemed to induce less cell death, compared to the results of TIGR4 (21.38 vs. 33.47 %, after a 5-h exposure; $P < 0.05$). Our data indicate that impaired pneumococcal CPS may increase biofilm formation and be involved in inhibition of virulence, possibly by influencing the gene expression.

L. Qin (✉) · Y. Imamura · H. Watanabe
Division of Infectious Diseases, Department of Infectious
Medicine, Kurume University School of Medicine,
67 Asahi-machi, Kurume, Fukuoka 830-0011, Japan
e-mail: braverok@hotmail.com; shin_ryou@med.kurume-u.ac.jp

Y. Kida · K. Kuwano
Division of Microbiology, Department of Infectious Medicine,
Kurume University School of Medicine, Fukuoka, Japan

Introduction

Streptococcus pneumoniae is an important human pathogen that is recognized as a major cause of community-acquired pneumonia, acute sinusitis, otitis media, meningitis, bacteremia, and other conditions. Since the first case of penicillin-resistant *S. pneumoniae* was reported in the 1970s, drug-resistant *S. pneumoniae* has spread all over the world. Consequently, the treatment of both invasive and chronic infections caused by *S. pneumoniae* has become an important issue [1–5]. Recently, *S. pneumoniae* was reported to form biofilms, which is thought to be a unique mechanism by which the pathogen escapes the host immune response and antimicrobial elimination [6–10]. Biofilms are highly structured, sessile microbial communities, characterized by bacteria attached to either a surface or interface, that are embedded in a matrix of extracellular polymeric substances. Hence, the rate at which bacteria attach to a surface is an important determinant of biofilm formation [11, 12]. *S. pneumoniae* are enveloped by capsule polysaccharides (CPSs). It is well known that pneumococcal CPS is usually synthesized by the Wzx/Wzy-dependent pathway, except for types 3 and 37, which are synthesized by the synthase pathway. The 5′-portion of the *S. pneumoniae* cps loci, encoding the first four genes (*cpsA–cpsD*), is common to most serotypes of *S. pneumoniae*, which are located at the chromosomal *cps* locus between *dexB* and *aliA* [13–15]. CpsA, which does not seem to be essential for encapsulation, has been shown to be a transcriptional activator of the cps locus in *Streptococcus agalactiae*. CpsB is a manganese-dependent phosphotyrosine-protein phosphatase that

🖄 Springer

is required to dephosphorylate CpsD. CpsC and CpsD are predicted to function together in polymerization and export of CPS in a fashion similar to ExoP in exopolysaccharide production in *Sinorhizobium meliloti* and Wzc from *Escherichia coli*. CpsC is required for CpsD tyrosine phosphorylation. CpsD is an autophosphorylating protein-tyrosine kinase, and point mutations in the *cpsD* gene attenuate its activity and regulate CPS production [6, 16, 17].

Expression of CPS is essential for systemic virulence because of its antiphagocytic properties, which has been well characterized [15, 18]. CPS was also reported to be involved in the adherence of pneumococci to host cells [9], and encapsulated clinical pneumococcal isolates were reported to have impaired biofilm formation [6]. The thickness of the CPS may also influence the degree of exposure of other important pneumococcal surface structures, such as the adhesins, which are required during the initial colonization phase. These results indicate that CPS may play an important role in pneumococcal pathogenicity and biofilm formation. Previous studies reported that recombinational exchange at the CPS biosynthetic locus may lead to frequent serotype changes [19], and strains with spontaneous CPS switching had even been detected in clinical trials [20, 21]. On the other hand, adherence and virulence protein A (*pavA*), the autolysin (*lytA*), the immunoglobulin A1 protease (*IgA1*), the ion transporters (*psaA* and *piaA*), the pneumococcal cytotoxin pneumolysin (*ply*), and pyruvate oxidase (*spxB*) were reported as a part of genes that were considered important in promoting carriage or disease [22–24]. Modification of CPS may also influence expression of these key genes during colonization and sequentially change the pathogenicity.

In the present study, we attempted to provide direct evidence to prove that impaired CPS enhances *S. pneumoniae* biofilm formation, and investigated the pathogenic diversities, as well as the mRNA expression of seven genes relevant to adherence and virulence in different life conditions.

Materials and methods

Bacterial strains, plasmid, media, and serotyping

The serotype 4 *S. pneumoniae* ATCC BAA-334 strain (TIGR4) [25], the genome of which had been sequenced, and the laboratory-derived TIGR4cps4D⁻ strain, were used in this study. Pneumococcal strains were grown on Trypticase soy agar (TSA II) supplemented with 5 % defibrinated rabbit blood (Becton-Dickinson, Sparks, MD, USA) at 37 °C in 5 % CO_2 for 18 h. A single colony was selected and used to inoculate brain heart infusion (BHI) broth, which was then cultured overnight. Serotype

identification of the strains was performed using a Pneumotest-Latex kit according to the manufacturer's instructions (Statens Serum Institut, Copenhagen, Denmark). Agglutination within 5–10 s was indicative of a positive serotype test. The plasmid pMPM-A4Ω (6.455 kb), which contained ampicillin and spectinomycin resistance genes as the selection markers, was kindly provided by the National Institute of Genetics (Shizuoka, Japan) [26].

Construction of cps4D disruption plasmid

Chromosomal DNA from pneumococcal isolates was prepared as previously described [27]. Briefly, DNA was extracted by suspending bacterial colonies in 50 μl distilled water, followed by boiling for 5 min. Polymerase chain reaction (PCR) was performed using Ex Taq DNA polymerase. *Cps4D* (SP_0349) was amplified in 50 μl, using 2 μl of pre-prepared bacterial lysate as the DNA template. The PCR profile included denaturation at 95 °C for 1 min, followed by 35 cycles of denaturation at 95 °C for 20 s, annealing at 55 °C for 20 s, extension at 72 °C for 20 s, and a final extension at 72 °C for 10 min. The following TIGR4cps4D⁻-specific primers were used: forward primer sequence [corresponding to TIGR4 (GenBank AE005672) *cps4D* nucleotides 127–156] 5′-CTC GAG CTC GAG GAT ATC ACG TTT ATT CGC CTC ACC TGT TGC-3′ (underlining indicates *Xho*I restriction site), and reverse primer sequence (corresponding to TIGR4 *cps4D* nucleotides 608–636 bp) 5′-AGA TCT AGA TCT GCA GAA GAA TAT TAC AAT GCC TTG TGT AC-3′ (underlining indicates *Bgl*II restriction site). The 484-bp PCR products were digested using *Xho*I and *Bgl*II and then cloned into a pMPM-A4Ω plasmid. The resultant plasmid was named pΔcps4D.

Transformation procedures

The transformation method used in this study was a modification of previously reported methods [28, 29]. In brief, an overnight culture of TIGR4 was diluted to an optical density of approximately 0.5 OD_{490} in competence medium [BHI broth containing 0.2 % bovine serum albumin (BSA) and 0.01 % $CaCl_2$] and aliquoted for storage at −80 °C after addition of 10 % glycerol. TIGR4 was transformed as follows. Competent cells (200 μl) were thawed, followed by addition of 20 μl pΔcps4D (43.25 μg/ml). The mixture was incubated at 37 °C for 2 h and then plated onto TSA II agar containing ampicillin (40 μg/ml) and streptomycin (40 μg/ml). Insertion of pΔcps4D into the *cps4D* gene was confirmed by PCR using PrimeSTAR GXL DNA Polymerase (Takara, Shiga, Japan). The PCR profile included denaturation at 98 °C for 3 min, followed by 30 cycles of

denaturation at 98 °C for 10 s, annealing at 55 °C for 15 s, extension at 68 °C for 9 min, and a final extension at 68 °C for 5 min. Primers were designed from the region 500 bp upstream and downstream of the cps4D gene: forward primer sequence (1833693–1836731), 5′-ATA ACC GGA CCT TCT GAA TC-3′; reverse primer sequence (1838421–1838441), 5′-GAA TAT ACG AGT ACC ACG CGA-3′.

Scanning electron microscopy (SEM)

Bacteria were incubated in 2.5 % glutaraldehyde for 1 h at room temperature. Cells were centrifuged at 1,500 rpm for 5 min, and the supernatant was decanted. After washing with 7.5 % sucrose (1 h), fixation was performed by incubation in 1 % OsO_4 [2 % OsO_4 was diluted with 7.5 % sucrose (1: 1)] for 1 h (4 °C). Specimens were continuously dehydrated by critical-point drying, which involves the replacement of water in the cells with graded ethanol from 50 % to 100 % and use of 100 % t-butyl alcohol for freeze drying. Samples were coated with gold in an ion-sputter coater and observed with an SEM (S-800, Hitachi, Tokyo, Japan) [30].

Transmission electron microscopy (TEM)

Bacteria were incubated in 2.5 % glutaraldehyde for 1 h at room temperature. Subsequently, the bacteria were washed for several hours in phosphate-buffered saline (PBS, pH 7.0) containing 7.5 % sucrose and then postfixed in 1 % OsO_4 for 1.5 h at 4 °C. The fluid was removed and the specimens were dehydrated in graded acetone (50–100 %), transferred into dibutyl glycidyl ether, and embedded in epoxy resin. Ultrathin sections (70 nm) were stained with uranyl acetate and lead citrate and examined using TEM (H-7000; Hitachi, Tokyo, Japan) [30].

Microtiter biofilm assay (MBA)

Biofilm formation by S. pneumoniae strains was assessed using 96-well (flat bottom) polystyrene (PST) microtiter dishes (NUNC, Roskilde, Denmark) as previously described [31]. Briefly, the concentration of bacteria was initially adjusted with brain–heart infusion (BHI) broth to a turbidity of 0.05 (OD_{490}). After a 24- or 48-h incubation, the culture medium containing planktonic cells was stained with 1 % crystal violet at room temperature. After strongly washing the medium with water three times, the dye bound to the biofilm was extracted with 230 μl 95 % ethanol for 15 min. The extracted dye was quantified by measuring the absorbance at 595 nm with a microplate reader. All strains were tested in triplicate, and the average ± SD of each experiment was calculated.

Biofilm growth in a continuous-flow chamber

Strains were grown to mature biofilms in a continuous-flow cell chamber as described by Davies et al. [32]. Strains were grown in BHI broth to the mid-log phase and then diluted to an optical density of 0.1 (OD_{490}). A 1 ml aliquot of the cell suspension, approximately $1 \times 10^{8-9}$ colony-forming units (CFU)/ml, was used to inoculate a flow-cell chamber (37 × 5 × 5 mm), followed by incubation at 37 °C for 2 h. During this incubation, bacteria were expected to tightly adhere to the glass coverslip. The chambers used in the present experiment were designed to reduce fluid shear on the biofilms relative to that induced by typical wells that are 1 mm deep. The chambers were subsequently incubated in BHI for 24 or 48 h at 37 °C under continuous flow (flow speed <500 μl/min).

Confocal laser scanning microscopy (CLSM)

Biofilm architecture was investigated by using inverted CLSM (Olympus, Tokyo, Japan) as described previously [31]. Pneumococcal biofilms were rinsed with PBS and then stained with Live/Dead BacLight from Invitrogen (Carlsbad, CA, USA). Cells with a compromised membrane that are considered to be dead or dying stain red, whereas cells with an intact membrane stain green. To ensure reproducibility, each experiment was performed in triplicate. Images were analyzed using FV10-ASW Viewer Ver. 1.7b (Olympus); projections through the x–y plane and the x–z plane were obtained.

RNA isolation

Pneumococcal strains were grown in BHI broth in 50-ml tubes for 24 h. Planktonic cells (approximately 10^7 CFU/ml) were recovered by centrifugation at 8,000 rpm for 5 min at 4 °C. A 15-ml aliquot of the cell suspension (approximately 1×10^6 CFU/ml) was inoculated into 150-cm^2 film-made lid tissue culture flasks (Iwaki, Japan) and cultured for 24 h. The culture medium was removed and the flasks were vigorously washed three times with PBS (−) buffer. The bottom of flasks to which biofilm had tightly adhered were scratched; then the cells were recovered using 200 μl of an RNA Stabilization Solution (Ambion, Japan). Total RNA was isolated using a commercial high-purity RNA isolation kit, following the manufacturer's manual (Roche, Mannheim, Germany). Finally, RNA of each sample was eluted in 100 μl RNase-free water. Quantification and crude quality assessment were done by a micro-volume spectrophotometer (Thermo Scientific, USA), and a visual examination on a 0.8 % ME

agarose gel in Tris–borate–ethylenediaminetetraacetic acid (EDTA) buffer stained with ethidium bromide. Aliquots of total RNA were stored at $-80\ °C$ until use.

Real-time PCR analysis

The qualified RNA was then used for cDNA synthesis, which was performed by random priming (Random 6 mers) on total RNA by using a real-time (RT)-PCR kit as described by the manufacturer (Takara, Japan). Genes (*pavA*, *lytA*, *IgA1*, *piaA*, *psaA*, *ply*, and *spxB*) relative to adherence and virulence were selected to test in the quantitative real-time PCR with SYBR green detection (Table 1). The primers were designed according to the published genomic sequence of TIGR4 (GenBank AE005672). Primer-pair efficiency was analyzed using varying concentrations of TIGR4-derived DNA template, and the C_T values obtained corresponded to the expected relative concentrations of template. The optimal concentrations of primers used in these studies were determined empirically in accordance with the manufacturer's instructions. Each reaction was conducted in duplicate two-step multiplex real-time PCRs with SYBR premix Ex Taq GC (TaKaRa, Japan) on a Real Time System TP800 (Takara, Japan). 16S ribosomal RNA (16S rRNA) served as an internal reference gene. The relative expression level was measured by using the $2^{-\Delta\Delta C_T}$ method described by Livak and Schmittgen [33].

Cytotoxicity detection assay

Prepared 100 μl medium (without antibiotics) containing BEAS-2B cells (human bronchial epithelium cells), about 10^5/ml for each well of a 96-well plate, was incubated for 48 h at 37 °C with 5 % CO_2. Bacteria were diluted to 10^5 CFU/ml for each strain. Then, 100 μl of each diluted bacteria suspension was added into previously prepared 96-well plates after removing the culture medium, except for the low control wells, and were then continually cultured for 24 h at the same condition. We quantitated the cytotoxicity in 96-well plates 24 h after infection using a Cytotoxicity Detection Kit (LDH) (Roche, Mannheim, Germany). Assay followed the manufacturer's protocol. In brief, 5 μl lysis solution was added to the high control wells and incubated for an additional 15 min; 100 μl reaction mixture was added to each well, and incubated for up to 30 min at room temperature. Finally, 50 μl stop solution was added to each well to stop the reaction. Optical density of each sample was measured at 490 nm by a microplate reader. All infection studies were tested in triplicate, and the average ± SD of each experiment was calculated.

Table 1 Primer sequences of housekeeping gene and genes relative to adhesion or virulence

Genes	Forward primer sequences (5′–3′)	Reverse primer sequences (5′–3′)	Accession number (gene ID)	Function	Size (bp)
16S[a] *rRNA*	TCTTGACATCCCTCTGACCGC	CCAACATCTCACGACACGAGC	SP rrnaA16S (929754)	16S ribosomal RNA	100
pavA	TCCACCAAGTGCCTAACGACC	GGGAGTCAGAGCCTTATCAAGCG	SP 0966 (931286)	Adherence and virulence protein A	95
lytA	CGGATTATCACTGGCGGAAAG	CAGGCACCATTATCAACAGGTCC	SP 1937 (931994)	Autolysin	100
IgA1	CAA CCT GAG ACT GGT GTA G	GTC ACT TAC TAC AGC TTC G	SP 1154 (931668)	Immunoglobulin A1 protease	96
piaA	CAGTTCATCTGATAAAGGAGACGG C	CTTCAAAGGCAGGAATAGTTGCT C	SP 0243 (930044)	Iron ABC transporter iron-binding protein	92
psaA	CACACGAATACGAACCACTTCCTG	GCATTGCCACCTGTTTCAAGG	SP 1650 (931186)	Manganese ABC transporter manganese-binding adhesion lipoprotein	97
ply	TCAAGAAGGCAGTCGCTTTACAG	AAGGTCGCAACTACATTGTCACG	SP 1923 (931915)	Pneumolysin	90
spxB	CAATCTACGGTATCCCATCAGGAAC	CGTGGCGAACTTGTAAGAAACG	SP 0730 (930680)	Pyruvate oxidase	90

[a] 16S rRNA was analyzed as the housekeeping gene

Statistical evaluation

Data were analyzed using the Student's paired t test. $P < 0.05$ was considered statistically significant.

Results

Construction of the CPS-impaired mutant TIGR4cps4D⁻

To confirm the role of CPS in *S. pneumoniae* biofilm formation, we constructed a CPS-impaired mutant. Several drug-resistant colonies were chosen from the selective blood agar plate containing ampicillin and streptomycin (40 μg/ml). Insertion of the DNA fragment within the *cps4D* gene was confirmed by PCR (Fig. 1a). In the wild-type TIGR4 strain, a 1,728-bp segment spanning 500 bp up- and downstream of the *cps4D* gene was amplified. By contrast, an 8,183-bp DNA fragment was amplified in TIGR4cps4D⁻, which confirmed insertion of the plasmid vector into the *cps4D* gene site.

Morphological characteristics were investigated. The TIGR4 colony phenotype observed using SEM was smooth or mucoid (Fig. 1b), and TEM showed the considerable thickness of the CPS (Fig. 1d). These results suggest that TIGR4 produced a considerable amount of CPS. By contrast, the CPS of the mutant TIGR4cps4D⁻ had a rough outer surface (Fig. 1c), and the amount of CPS-related material evenly distributed over the cell surface was very small (Fig. 1e). These observations prove that the *cps4D* gene was mutated and that TIGR4cps4D⁻ produced an impaired CPS.

A mutation in the *cps4D* gene affected CPS expression and, consequently, may change the serotype. Therefore, the serotypes of TIGR4 and TIGR4cps4D⁻ were determined using a rapid latex agglutination test, as described in "Materials and methods." According to the protocol, agglutination of latex pool sera A and R was observed simultaneously, which indicated that TIGR4 was serotype 4. By contrast, no agglutination was observed for TIGR4cps4D⁻. This result indicates that secretion of CPS was interrupted by the DNA insertion into TIGR4cps4D⁻.

Characterization of biofilm formation

Using an in vitro batch biofilm assay performed in 96-well microtiter plates, both TIGR4 and mutant TIGR4cps4D⁻ were proven capable of biofilm formation (Fig. 2). There were no significant differences in planktonic growth (OD_{490}) between strains on day 1, and even TIGR4 seemed to grow better than TIGR4cps4D⁻ on day 2. How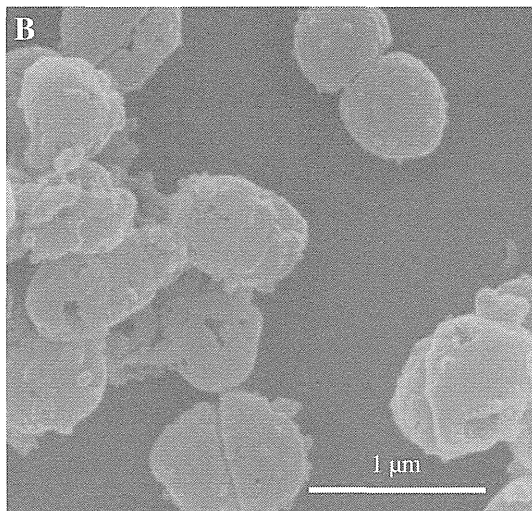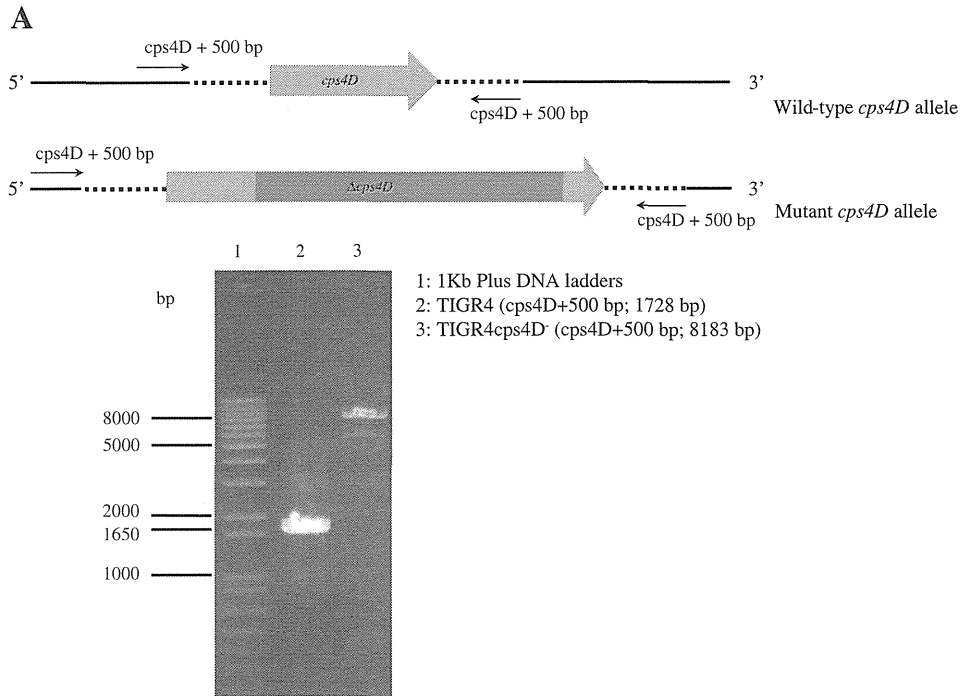ever, there were differences in the optical densities of the biofilms. The mean OD_{595} of TIGR4cps4D⁻ was 1.77 on day 1 and 1.74 on day 2, whereas that of TIGR4 was 0.76 and 0.33, respectively. These results indicate TIGR4cps4D⁻ was more capable of forming a biofilm in vitro than its parental strain.

Next, biofilms were grown in a continuous-flow cell system for 24 or 48 h under once-through flow conditions. Biofilm architectures were visualized at 400× magnification after staining to show the viable cells in green and dead cells in red fluorescence. Flow-cell experiments were performed in triplicate, as described in "Materials and methods." The CLSM images depicted in Fig. 3 show horizontal three-dimensional (3-D) reconstructions scanned in the *x–y* and *x–z* planes. The results are typical for biofilms after 24 h of culture. Each image shows a mature biofilm structure composed of a large cluster of cells. The CPS-impaired TIGR4cps4D⁻ formed a biofilm with a depth of ~ 12.22 μm (Fig. 3b), which was a much higher density and thickness than the biofilm formed by TIGR4 with wild-type CPS (≈ 6.29 μm) (Fig. 3a). Data observed after 48 h of culture showed congruent results (data not shown).
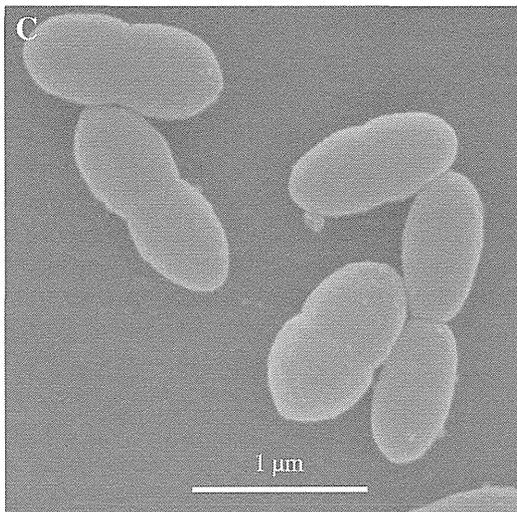
Despite its destructive nature, scanning electron microscope (SEM) observations provided useful information on the different cellular morphologies present in the biofilms (Fig. 3c, d). The definition of biofilm was the recognition of slime and a multilayer formation of bacteria. As in biofilms formed under static conditions, the TIGR4 strain was seen to compose a dense aggregate of individual bacteria (Fig. 3c), whereas the TIGR4cps4D⁻ strain was recognized to contribute a 3-D conformation structure similar to biofilms observed at 24 h. The pellicle was formed by the biofilm matrix at the top of the biofilm structure of each strain, and fibrils extending between bacteria were also observed from both strains at 48 h. The TIGR4cps4D⁻ strain seemed to form a denser network of cells, and the biofilms occupying the coverslip were larger and thicker (Fig. 3d).
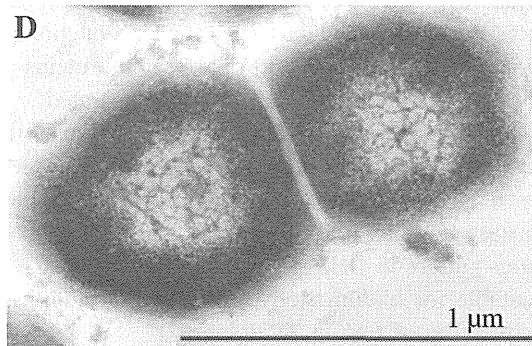
Real-time PCR analysis

Total bacterial RNA extracted from TIGR4 and the mutant TIGR4cps4D⁻ grown under planktonic conditions and biofilms were used to investigate the in vitro expression levels of the seven genes (*pavA*, *lytA*, *IgA1*, *piaA*, *psaA*, *ply*, and *spxB*). Compared to TIGR4, of the seven genes analyzed, four genes (*pavA*, *piaA*, *ply*, and *spxB*) showed increased expression of 0.9×10^1-, 1.4×10^1-, 2.9×10^1-, and 0.7×10^1-fold change in TIGR4cps4D⁻ under planktonic conditions, respectively, whereas the expressions of *lytA*, *IgA1*, and *psaA* were decreased 1.9×10^{-5}-, 2.4×10^{-5}-, and 3.2×10^{-3} fold, respectively (Fig. 4a). Furthermore, under biofilm conditions, *pavA*, *piaA*, *psaA*, *ply*, and *spxB* of TIGR4cps4D⁻ showed increased expression that was
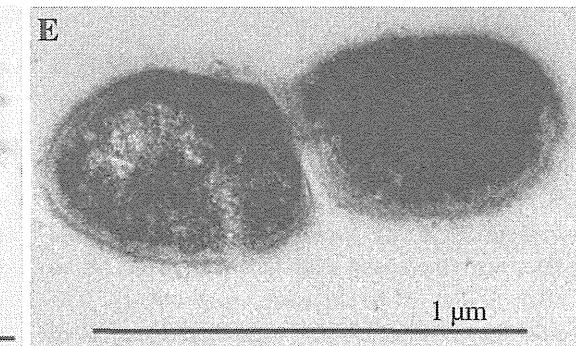
A

Wild-type *cps4D* allele

Mutant *cps4D* allele

1: 1Kb Plus DNA ladders
2: TIGR4 (cps4D+500 bp; 1728 bp)
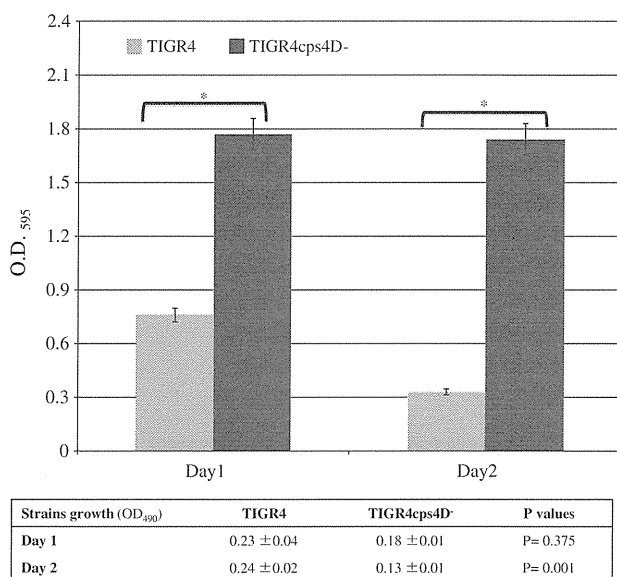3: TIGR4cps4D⁻ (cps4D+500 bp; 8183 bp)

TIGR4

TIGR4cps4D⁻

TIGR4

TIGR4cps4D⁻

◀ **Fig. 1 a** Confirmation of the mutant by polymerase chain reaction (PCR). Primers were designed to span a region 500 bp up- and downstream from the *cps4D* gene for confirmation of the capsular polysaccharide-impaired mutant. **b, c** Capsular polysaccharide (CPS) on the cell surface of TIGR4 and TIGR4cps4D⁻ observed by scanning electron microscopy (SEM). A representative bacterium is shown for TIGR4 and TIGR4cps4D⁻, respectively. **d, e** CPS on the cell surface of TIGR4 and TIGR4cps4D⁻ observed by transmission electron microscopy (TEM). A representative bacterium is shown for TIGR4 and TIGR4cps4D⁻, respectively. **b, c, d, e** ×30,000

Strains growth (OD$_{490}$)	TIGR4	TIGR4cps4D⁻	P values
Day 1	0.23 ±0.04	0.18 ±0.01	P= 0.375
Day 2	0.24 ±0.02	0.13 ±0.01	P= 0.001

Fig. 2 Biofilm formation capacity of TIGR4 and TIGR4cps4D⁻. Bacterial cells were cultured in BHI broth at 37 °C for 24 and 48 h, and the growths were investigated before assay. *Gray and black bars* indicate the biofilm formation of TIGR4 and TIGR4cps4D⁻, respectively. Results are average ± SD of three independent experiments. *$P < 0.0001$

4.9×10^2-, 2.4×10^3-, 3.2×10^1-, 4.7×10^2-, and 3.6×10^1-fold higher compared to TIGR4, except the expressions of *lytA* and *IgA1*, which were 1.9×10^{-5}- and 9.7×10^{-5}-fold lower, respectively (Fig. 4b).

## Pathogenic effect of TIGR4cps4D⁻ infection on viability of BEAS-2B cells

To ensure the pathogenicity of the TIGR4cps4D⁻ strain in our experiments, a cytotoxicity detection assay was performed. BEAS-2B cell death was evaluated by LDH release, following an infection with TIGR4 and TIGR4cps4D⁻ after an incubation of 5 or 24 h (Fig. 5). TIGR4 increased cell death from 33.47 to 45.41 %, and TIGR4cps4D⁻ also increased cell death from 21.38 to 31.44 %, after 5 and 24 h exposure, respectively. The figure reveals that TIGR4cps4D⁻ significantly reduced BEAS-2B cell death compared to TIGR4, when observed after 5 or 24 h exposure ($P < 0.05$).

Discussion

In this study we observed mature biofilms produced by both TIGR4 and its CPS-impaired mutant TIGR4cps4D⁻. These data provide direct evidence that *S. pneumoniae* forms mature biofilms in vitro. Furthermore, because TIGR4cps4D⁻ formed a larger and thicker biofilm than did its parental strain, loss of CPS has the potential to promote biofilm formation (or possibly quicken the biofilm formation in the early adherence). Previous studies reported that a series of derivatives from the clinical or laboratory-originated pneumococcal isolates expressed comparable amounts of CPS that differed from that of the parental strain, and some of these CPS exhibited reduced biofilm formation [6]. These results indicate that CPS is actually involved in biofilm formation. In our study, electron microscopy confirmed the disruption of CPS secretion, which subsequently promoted biofilm formation. This interesting finding gives the direct evidence to reveal the relatedness of CPS expression and pneumococcal biofilm formation. CPS was reported to block the function of a self-recognizing adhesin 43 through physical shielding and sterically prevent receptor–target recognition of short bacterial adhesins, and this negative interference affects the ability of bacteria adherence during the initial colonization phase.

psaA encodes a surface-exposed common 37-kDa multifunctional lipoprotein detected on all known serotypes of *S. pneumoniae*. It also plays a major role in pneumococcal attachment to the host cell and virulence [34]. In our study, alternating expression was detected for *psaA* under planktonic conditions and biofilms. The higher expression level of *psaA* in TIGR4cps4D⁻ in biofilms indicated that impaired CPS might influence *psaA* expression, but this should be tested by further similar experiments with the addition of exogenous CPS to non-CPS-expressing TIGR4cps4D⁻ or co-culture with other bacterial species that produce biofilms. Our results indicated that the TIGR4 strain formed fewer biofilms than did the CPS-impaired mutant, which may be caused by either sterical shielding of adhesion proteins by the CPS or CPS production interfering with synthesis or transport of adhesion proteins to the cell surface, as Schembri et al. [35] demonstrated.

In the previous studies, biofilms were most often grown in Todd–Hewitt broth [6, 8–10] whereas very few studies used BHI broth as the culture medium. In our studies, mature biofilms were observed after 24 or 48 h of continuous culture in BHI broth, which proved that BHI is also suitable for biofilm study. Although in biofilms the gene expression of *lytA* in TIGR4cps4D⁻ was 1.9×10^{-5}-fold lower than TIGR4, we noticed that the number of dead pneumococcal cells was increased in the TIGR4cps4D⁻ biofilms (Fig. 3b). The reason remains unclear; the

A   TIGR4   Z: 6.29 μm

B   TIGR4cps4D⁻   Z: 12.22 μm
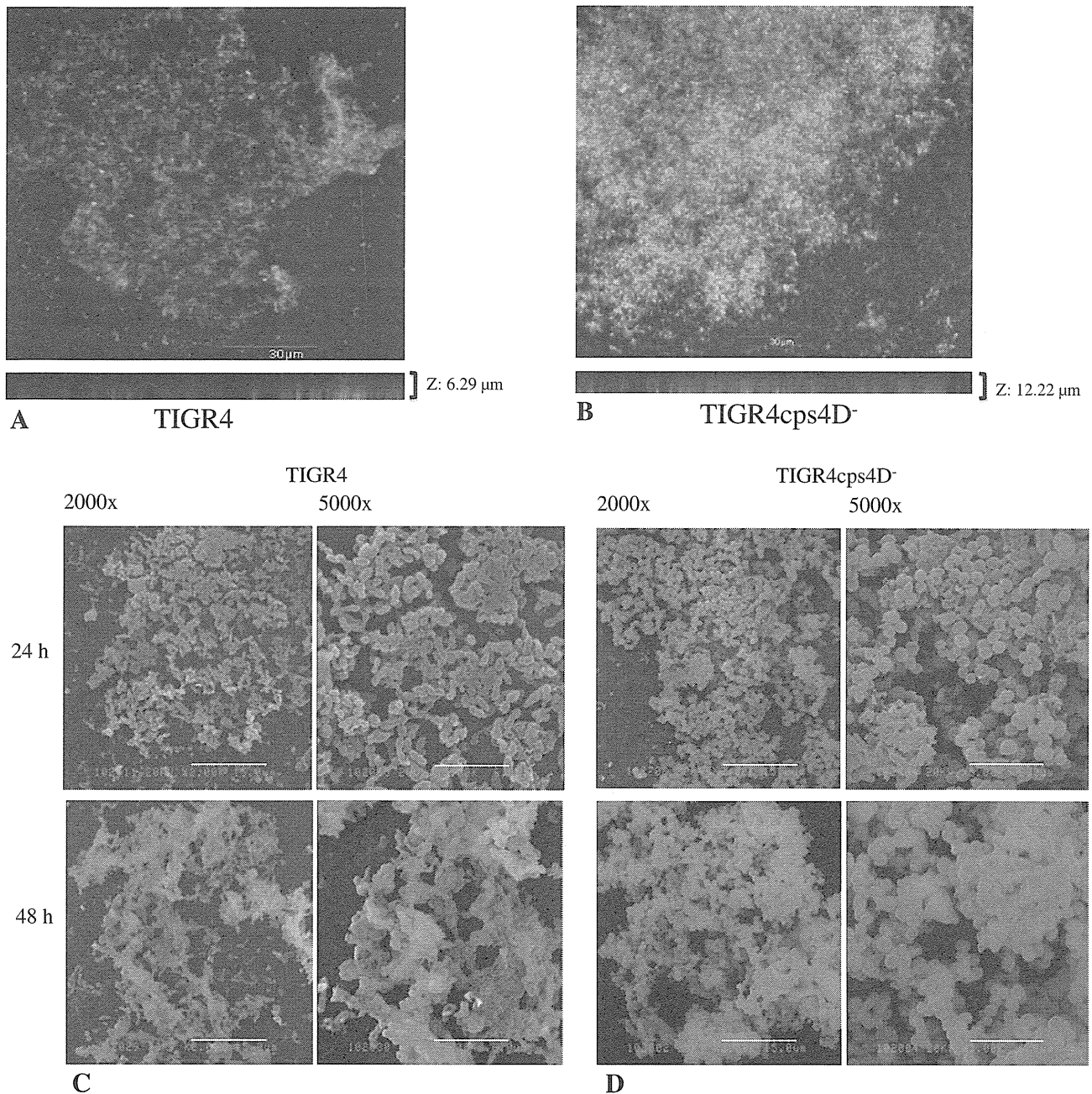
Fig. 3 Biofilm architecture with confocal laser scanning microscopy (CLSM) and SEM visually observed after 24 h of culture. CLSM images (a, b) show the x–y and x–z planes. Flow-cell experiments were performed in triplicate as described in "Materials and methods."

Bars 30 μm. ×400. Biofilm architecture visually observed with SEM (c, d) after 24 and 48 h of culture, respectively; SEM images were taken at 2,000× and 5,000× for each strain

effective inhibition of pneumococcal autolysin is thought to be a priority of future pneumococcal biofilm studies. Allegrucci and Sauer [9] reported the biofilm development process occurred in three distinct stages, and biofilm viable cell counts and total protein concentration increased steadily over the course of biofilm development, reaching $\sim 8 \times 10^8$ cells and ~ 15 mg protein per biofilm after 9 days of biofilm growth. However, another study [7]

reported that the total biofilm cell counts stabilized after 21 h, at approximately 10^5 cells/cm^2, whereas viable counts decreased as the biofilm aged. Thus, we think it should not be easy to judge whether pneumococcal biofilms detach after a longer period of time. As the biofilm seemed to be affected by many factors such as culture condition, medium, and strains, more studies should be focused on this aspect.
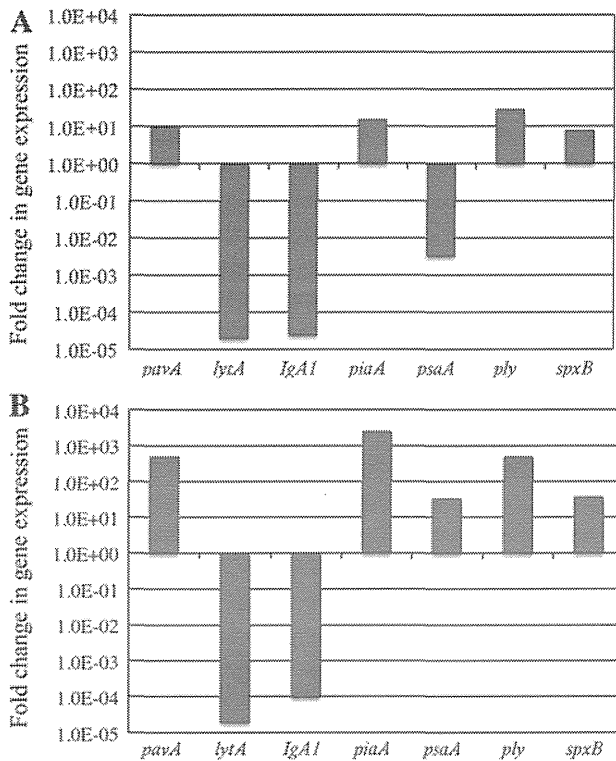
Fig. 4 Expression level of genes relative to adherence or virulence in TIGR4cps4D⁻ compared to TIGR4. Strains were grown in BHI broth (a) to the stationary phase, and total RNA was analyzed by real-time PCR analysis using primers specific for *pavA*, *lytA*, *IgA1*, *piaA*, *psaA*, *ply*, and *spxB*. Gene expression of RNA isolated from biofilms (b) was analyzed
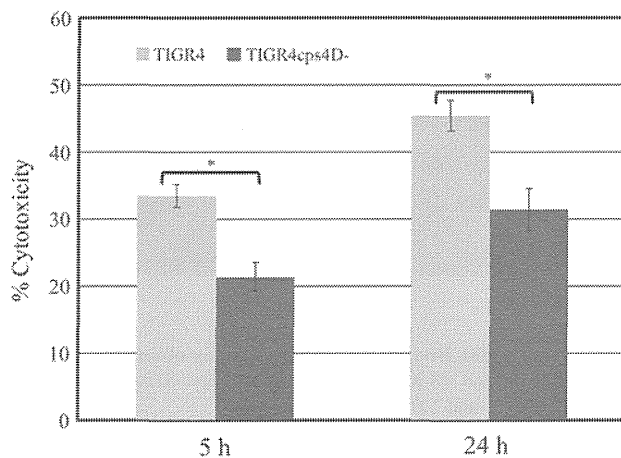
Fig. 5 BEAS-2B cells were assessed for cytotoxicity following an infection with TIGR4 and TIGR4cps4D⁻ strains. Cytotoxicity was quantitated based on the measurement of LDH activity released from damaged cells after 5 and 24 h culture, respectively. Results are average ± SD of three independent experiments. *$P < 0.05$

S. pneumoniae is capable of producing CPS, which is structurally distinct for each of 90 known serotypes and is essential for pneumococcal virulence [15, 36]. Maximal

expression of CPS is essential for systemic virulence because of its antiphagocytic properties. A previous study reported that a *cps2D*-deleted D39 strain that produced a reduced amount of CPS was avirulent [37]. In the present study, the CPS-impaired mutant seemed to be reduced in pathogenicity compared to its parental strain. We also investigated the expression of seven genes based on their putative functions relative to adherence and virulence. *lytA* encoded autolysin, which may play a direct role in virulence by mediating the release of cell-wall components shown to be highly inflammatory, and in pathogenesis by mediating cell lysis and the subsequent release of virulence factors, such as pneumolysin. As a result, much higher expressions were detected for *lytA* and *IgA1* in TIGR4 under both planktonic conditions and biofilms. Previous studies found that disruption of the gene encoding the autolysin LytA reduces competence-induced cell lysis two- to fourfold [38], and interruption of the chromosomal gene resulted in loss of expression of an approximately 200-kDa protein and complete elimination of detectable IgA1 protease activity [39]. These results suggested that the interrupted *lytA* and *IgA1* expression might be responsible for the reduced pathogenicity of TIGR4cps4D⁻. As is well known, pneumolysin was reported as an important virulence factor, contributing to multiple stages of the pathogenic process, and it is also involved in eliciting an immune response from the host. The cytotoxic characteristic of pneumolysin facilitates progression of diseases by inhibiting ciliary beating in the human respiratory epithelium, and also acts by disrupting tight junctions between epithelial cells. Additionally, numerous studies demonstrated that mutants lacking pneumolysin showing reduced replication and survival in the bloodstream of infected animals [40, 41]. Higher expression was detected for *ply* in TIGR4cps4D⁻, with reduced cytotoxicity. Because pneumolysin production is regulated at a posttranscriptional level, it may be regulated independently of environmental stimuli, with the niche influencing the release of the toxin rather than its transcription or translation, as suggested by LeMessurier et al. [22]. There are some limitations of the present study. We hypothesize the CPS product, expressions of *pavA*, *lytA*, *IgA1*, *piaA*, *psaA*, *ply*, and *spxB*, played the important role in inducing cytotoxicity, but we did not investigate the protein/transcriptional levels of pneumolysin, as well as the other genes; thus, we could not demonstrate the key factor expressing cytotoxicity in this experiment or how impaired CPS affects the expression of virulence genes. Furthermore, whether TIGR4cps4D⁻ was able to reduce pathogenicity after adherence to epithelial cells or tissues, and then formed mature biofilms by avoiding the clearance of host immune responses, has not been investigated. Thus, an animal model is thought to be necessary for future work.

The biofilm matrix was reported to be regulated by CPS, protein components, and other extracellular molecules. Pneumococci with different serotypes have different surface properties that may promote (or hinder) biofilm formation and may be very important for the survival of pneumococci in different host environments. Hammerschmidt et al. [42] found invasive pneumococci exhibited an enhanced capacity to adhere and invade epithelial cells, appearing to cause a reduction in capsular material, which potentially increases biofilm formation. If invasive pneumococci acquire enhanced ability to form biofilms, their elimination would become difficult, with subsequent serious clinical implications. Variations in CPS may result in different biofilm phenotypes. Therefore, screening of strains that form biofilms with vaccine serotypes is important not only for development of new vaccine candidates but for reevaluation of existing pneumococcal vaccines, e.g., a 23-valent polysaccharide vaccine, or a 7-valent conjugated vaccine.

The present study demonstrated that CPS as a surface structure seems to be essential for regulation of biofilm development and virulence. The artificial disruption of CPS that increased biofilm formation may be caused by interference with the initial process of attachment in pneumococcus and subsequent biofilm development.

Conflict of interest We declare that none of the authors has financial arrangements with any company whose product is mentioned prominently in this manuscript nor with any company making a competing product.

References

1. Fang GD, Fine M, Orloff J, Arisumi D, Yu VL, Kapoor W, et al. New and emerging etiologies for community-acquired pneumonia with implications for therapy. A prospective multicenter study of 359 cases. Medicine (Baltim). 1990;69:307–16.

2. Appelbaum PC. Antimicrobial resistance in *Streptococcus pneumoniae*: an overview. Clin Infect Dis. 1992;15:77–83.

3. Linares J, Pallares R, Alonso T, Perez JL, Ayats J, Gudiol F, et al. Trends in antimicrobial resistance of clinical isolates of *Streptococcus pneumoniae* in Bellvitge Hospital, Barcelona, Spain (1979–1990). Clin Infect Dis. 1992;15:99–105.

4. Rello J, Rodriguez R, Jubert P, Alvarez B. Severe community-acquired pneumonia in the elderly: epidemiology and prognosis. Study Group for Severe Community-Acquired Pneumonia. Clin Infect Dis. 1996;23:723–8.

5. Restrepo MI, Jorgensen JH, Mortensen EM, Anzueto A. Severe community-acquired pneumonia: current outcomes, epidemiology, etiology, and therapy. Curr Opin Infect Dis. 2001;14:703–9.

6. Moscoso M, Garcia E, Lopez R. Biofilm formation by *Streptococcus pneumoniae*: role of choline, extracellular DNA, and capsular polysaccharide in microbial accretion. J Bacteriol. 2006;188:7785–95.

7. Donlan RM, Piede JA, Heyes CD, Sanii L, Murga R, Edmonds P, et al. Model system for growing and quantifying *Streptococcus pneumoniae* biofilms in situ and in real time. Appl Environ Microbiol. 2004;70:4980–8.

8. Allegrucci M, Hu FZ, Shen K, Hayes J, Ehrlich GD, Post JC, et al. Phenotypic characterization of *Streptococcus pneumoniae* biofilm development. J Bacteriol. 2006;188:2325–35.

9. Allegrucci M, Sauer K. Characterization of colony morphology variants isolated from *Streptococcus pneumoniae* biofilms. J Bacteriol. 2007;189:2030–8.

10. McEllistrem MC, Ransford JV, Khan SA. Characterization of in vitro biofilm-associated pneumococcal phase variants of a clinically relevant serotype 3 clone. J Clin Microbiol. 2007;45:97–101.

11. Costerton JW, Stewart PS, Greenberg EP. Bacterial biofilms: a common cause of persistent infections. Science. 1999;284:1318–22.

12. Wolcott RD, Ehrlich GD. Biofilms and chronic infections. JAMA. 2008;299:2682–4.

13. Kolkman MA, van der Zeijst BA, Nuijten PJ. Diversity of capsular polysaccharide synthesis gene clusters in *Streptococcus pneumoniae*. J Biochem (Tokyo). 1998;123:937–45.

14. Garcia E, Llull D, Munoz R, Mollerach M, Lopez R. Current trends in capsular polysaccharide biosynthesis of *Streptococcus pneumoniae*. Res Microbiol. 2000;151:429–35.

15. Bentley SD, Aanensen DM, Mavroidi A, Saunders D, Rabbinowitsch E, Collins M, et al. Genetic analysis of the capsular biosynthetic locus from all 90 pneumococcal serotypes. PLoS Genet. 2006;2:e31.

16. Morona JK, Paton JC, Miller DC, Morona R. Tyrosine phosphorylation of CpsD negatively regulates capsular polysaccharide biosynthesis in *Streptococcus pneumoniae*. Mol Microbiol. 2000;35:1431–42.

17. Morona JK, Morona R, Miller DC, Paton JC. Mutational analysis of the carboxy-terminal (YGX)4 repeat domain of CpsD, an autophosphorylating tyrosine kinase required for capsule biosynthesis in *Streptococcus pneumoniae*. J Bacteriol. 2003;185:3009–19.

18. Jiang SM, Wang L, Reeves PR. Molecular characterization of *Streptococcus pneumoniae* type 4, 6B, 8, and 18C capsular polysaccharide gene clusters. Infect Immun. 2001;69:1244–55.

19. Coffey TJ, Enright MC, Daniels M, Morona JK, Morona R, Hryniewicz W, et al. Recombinational exchanges at the capsular polysaccharide biosynthetic locus lead to frequent serotype changes among natural isolates of *Streptococcus pneumoniae*. Mol Microbiol. 1998;27:73–83.

20. Nesin M, Ramirez M, Tomasz A. Capsular transformation of a multidrug-resistant *Streptococcus pneumoniae* in vivo. J Infect Dis. 1998;177:707–13.

21. Tomasz A. New faces of an old pathogen: emergence and spread of multidrug-resistant *Streptococcus pneumoniae*. Am J Med. 1999;107:55S–62S.

22. LeMessurier KS, Ogunniyi AD, Paton JC. Differential expression of key pneumococcal virulence genes in vivo. Microbiology. 2006;152:305–11.

23. Mortier-Barriere I, de Saizieu A, Claverys JP, Martin B. Competence-specific induction of recA is required for full recombination proficiency during transformation in *Streptococcus pneumoniae*. Mol Microbiol. 1998;27:159–70.

24. Weiser JN, Bae D, Fasching C, Scamurra RW, Ratner AJ, Janoff EN. Antibody-enhanced pneumococcal adherence requires IgA1 protease. Proc Natl Acad Sci USA. 2003;100:4215–20.

25. Tettelin H, Nelson KE, Paulsen IT, Eisen JA, Read TD, Peterson S, et al. Complete genome sequence of a virulent isolate of Streptococcus pneumoniae. Science. 2001;293:498–506.

26. Mayer MP. A new set of useful cloning and expression vectors derived from pBlueScript. Gene (Amst). 1995;163:41–6.

27. Qin L, Watanabe H, Yoshimine H, Guio H, Watanabe K, Kawakami K, et al. Antimicrobial susceptibility and serotype distribution of Streptococcus pneumoniae isolated from patients with community-acquired pneumonia and molecular analysis of multidrug-resistant serotype 19F and 23F strains in Japan. Epidemiol Infect. 2006;134:1188–94.

28. Yother J, McDaniel LS, Briles DE. Transformation of encapsulated Streptococcus pneumoniae. J Bacteriol. 1986;168:1463–5.

29. Berry AM, Yother J, Briles DE, Hansman D, Paton JC. Reduced virulence of a defined pneumolysin-negative mutant of Streptococcus pneumoniae. Infect Immun. 1989;57:2037–42.

30. Inokuchi T, Yokoyama R, Higashi R, Takahashi Y, Miyajima S. Ultrastructure of the perineurial cell of the sciatic nerve in rats—a transmission and scanning electron microscopic study. Kurume Med J. 1991;38:221–32.

31. Kaji C, Watanabe K, Apicella MA, Watanabe H. Antimicrobial effect of fluoroquinolones for the eradication of nontypeable Haemophilus influenzae isolates within biofilms. Tohoku J Exp Med. 2008;214:121–8.

32. Davies DG, Parsek MR, Pearson JP, Iglewski BH, Costerton JW, Greenberg EP. The involvement of cell-to-cell signals in the development of a bacterial biofilm. Science. 1998;280:295–8.

33. Livak KJ, Schmittgen TD. Analysis of relative gene expression data using real-time quantitative PCR and the 2(-Delta Delta C(T)) method. Methods. 2001;25:402–8.

34. Rajam G, Anderton JM, Carlone GM, Sampson JS, Ades EW. Pneumococcal surface adhesin A (PsaA): a review. Crit Rev Microbiol. 2008;34:163–73.

35. Schembri MA, Dalsgaard D, Klemm P. Capsule shields the function of short bacterial adhesins. J Bacteriol. 2004;186:1249–57.

36. Martens P, Worm SW, Lundgren B, Konradsen HB, Benfield T. Serotype-specific mortality from invasive Streptococcus pneumoniae disease revisited. BMC Infect Dis. 2004;4:21.

37. Morona JK, Miller DC, Morona R, Paton JC. The effect that mutations in the conserved capsular polysaccharide biosynthesis genes cpsA, cpsB, and cpsD have on virulence of Streptococcus pneumoniae. J Infect Dis. 2004;189:1905–13.

38. Kausmally L, Johnsborg O, Lunde M, Knutsen E, Havarstein LS. Choline-binding protein D (CbpD) in Streptococcus pneumoniae is essential for competence-induced cell lysis. J Bacteriol. 2005;187:4338–45.

39. Wani JH, Gilbert JV, Plaut AG, Weiser JN. Identification, cloning, and sequencing of the immunoglobulin A1 protease gene of Streptococcus pneumoniae. Infect Immun. 1996;64:3967–74.

40. Boulnois GJ, Paton JC, Mitchell TJ, Andrew PW. Structure and function of pneumolysin, the multifunctional, thiol-activated toxin of Streptococcus pneumoniae. Mol Microbiol. 1991;5:2611–6.

41. Steinfort C, Wilson R, Mitchell T, Feldman C, Rutman A, Todd H, et al. Effect of Streptococcus pneumoniae on human respiratory epithelium in vitro. Infect Immun. 1989;57:2006–13.

42. Hammerschmidt S, Wolff S, Hocke A, Rosseau S, Muller E, Rohde M. Illustration of pneumococcal polysaccharide capsule during adherence and invasion of epithelial cells. Infect Immun. 2005;73:4653–67.

インフルエンザ（H1N1）2009発生時に地域に密着して実施した
実験室内診断症例の検討

久留米大学医学部感染医学講座臨床感染医学部門

今村　宜寛　　濱田　信之　　原　　好勇
柏木　孝仁　　渡邊　　浩

要　旨

　2009年の所謂新型インフルエンザアウトブレイクに対して，我々は地域に密着した検査体制を敷き，独自のプライマーを使ったRT-PCR法によるインフルエンザ（H1N1）2009ウイルス遺伝子の検出およびウイルス分離を行った．インフルエンザ疑いの患者30名中ペア血清が採取できた3名では抗体価は回復期で4倍以上の上昇を認め，当該ウイルスの感染が血清学的に証明された．さらに分離ウイルスを使用して，他機関に依頼することなく，赤血球凝集抑制反応（HI）を独自に実施し，ワクチン接種前の健常成人（24～60歳）血清のHI抗体価を調べた．その結果，ほとんどが抗体を持たなかったが，2名だけ低値の抗体を保有していることがわかった．ここで構築した独自の検査体制とその成果は，地方都市の診療所や病院での感染症診療に寄与し，さらにこれらの対応過程は将来起こるかもしれないインフルエンザを含んだ新型感染症パンデミック時のモデルとなると考える．

〔感染症誌　87：368～374，2013〕

序　文

　インフルエンザ（H1N1）2009は，2009年4月に米国Center for Disease Control and Prevention（CDC）により豚インフルエンザのヒトへの伝播として最初に報告された[1]．4月下旬になるとWorld Health Organization（WHO）は，本来高病原性鳥インフルエンザの流行を想定していた対策の枠組みを急遽当該流行に適用し，パンデミックインフルエンザのフェーズ5であると宣言した（後にフェーズ6が宣言された）[2]．このため5月に日本で最初の症例が神戸で報告されると，一時的に全国規模で医療も巻き込んだ大混乱に陥った．しかし，流行が全国に拡大していくうちに次第に落ち着きを取り戻した[3]．この間，疾患の特徴も次第に明らかにされ，症候は季節性のものと大差はないこと，若年者に感染が多い傾向にあることなどが明らかとなった．これは抗体保有率が高齢者では60％以上に対し，若年者（18～40歳）では6％程

度であることが関連していると考えられた[4][5]．

　ところで当該インフルエンザウイルスに対する既存の迅速診断キットは感度が50～70％といわれ[6]～[8]，感染防御のための検査として不十分と思われた．一方，より感度の高いRT-PCR法は，県などの公的機関での検査に限られ，一般の外来患者などでの対応は不十分であった．さらに当該ウイルスが行政上新型インフルエンザウイルスとされ，実質上P3施設での取扱いを国が求めたことも検査対応の遅れにつながった．

　本研究は，日本中が大混乱に陥りそれが終息する時期にあたる2009年5月より2010年1月までに，当該施設に検査依頼のあった重症例を含む患者検体について，インフルエンザ（H1N1）2009の検査を行った症例の報告である．流行の初期段階で米国CDCはそのホームページに米国最初の分離株の全塩基配列を公開した．そこで我々は独自にプライマーを設計し，それを使用したRT-PCR法により検査を行った．またP3施設内でウイルス分離を試み，分離されたウイルスをHI試験の攻撃抗原として使い，患者の血清抗体価の有無を調べた．

材料および方法

本研究は久留米大学倫理委員会の承認を得た（研究番号 12241）. また以下の操作は P3 実験室にて行った.

1. インフルエンザウイルス抗原の検出

2009 年 5 月 7 日〜2010 年 1 月 19 日までに当該施設に新型インフルエンザ検査依頼のあった熱発患者の 30 検体. 患者の鼻腔ぬぐい液をインフルエンザウイルス迅速抗原検出キット（エスプライン A & B-N, 富士レビオ）の検査材料とした.

2. インフルエンザウイルス遺伝子の検出及び判別

24 時間検査体制を 2009 年 5 月 7 日から 2009 年 11 月 6 日までの半年間とし, 4 名のスタッフを 2 班に分け, 7 日間を 1 クールとし検査を行った.

鼻腔ぬぐい液から QIAmpRNA 抽出キット（Qiagen）を用いてウイルス RNA を抽出し, 逆転写酵素反応（Superscript II reverse transcriptase, Invitrogen）; 45℃ 60 分, 75℃ 5 分を行い, 1st PCR（Ex-Taq, TAKARA）を 98℃ 10 秒, 55℃ 20 秒, 72℃ 90 秒を 25 サイクル行い続いて 2nd PCR を同じ条件で行った. プライマーの配列は Table 1 に示した. アガロース電気泳動を行い, 予想されるバンドが検出された場合, そのバンドを切り出し（Ultra Clean, MO-BIO）, ダイレクトシークエンシング（Big Dye terminator cycle sequencing kit および ABI prism 310 sequencer, ABI）により塩基配列を決定し, BLAST 検索によりウイルスの判別を行った.

3. ウイルス分離

迅速診断キットおよび RT-PCR による検査結果が共に陽性の鼻腔ぬぐい液を 3,000 回転, 10 分間遠心後, MDCK 及び CaCo-2 細胞の培養 2 日目に接種し 1 時間吸着させた後, トリプシン 1μg/mL（Sigma）を添加した無血清イーグル MEM（Nissui）中で CO_2 インキュベーターにて 37℃ で培養した. 1 代目は盲継代として 5 日目にハーベストを行い 1 回凍結融解し遠心上清を上と同様に MDCK 及び CaCo-2 細胞に接種し 2 代目継代とした. 毎日観察を行い CPE のみられた培養液を −80℃ で凍結した. 融解したのち, 4℃, 10 分 3000 回転遠心した上清に対して赤血球凝集反応陽性確認し, ウイルス分離液とした.

4. 赤血球凝集反応（HA）

96 穴のプレートを用いて第 1 穴にリン酸緩衝液（PBS）を 90μL, 第 2 穴以降は 50μL 分注し, 第 1 穴に分離ウイルス 10μL を分注混和, 50μL を 2 穴目に分注混和, 以後 2 倍階段希釈を行った. あらかじめ PBS で 3 回洗浄を行った 0.5% 七面鳥血球を 50μL 加え混和後, 室温に 1 時間放置し判定した. 凝集した最大希釈倍数を HA 価とした.

5. 赤血球凝集抑制試験（HI）

血清に RDE（デンカ生研）を 3 倍量入れ, 56℃ 30 分の非働化処理を行った. これらの血清を 10 倍〜1,280 倍まで 2 倍階段希釈を行ったのちウイルス抗原（4HA 価/50μL）を 25μL 等量加えた後, 室温で 30 分置いた. この混合液に 0.5% 七面鳥血球を 50μL 加え室温で 1 時間反応させ判定した. 凝集を完全に阻止した最大希釈倍数を HI 価とした. HI 価≧1：40 を感染防御レベルとした.

成 績

1. 症例の詳細（Table 2）

2009 年 5 月 7 日より 2010 年 1 月 19 日までに検査依頼は 30 検体であった. 患者の年齢は 5 歳〜66 歳であり, 男性 8 名, 女性 12 名, 記録なしが 10 名であった. 渡航歴では米国帰国者 1 名, 沖縄旅行者 2 名であり, その他は記録がなかった. 迅速診断キットでは, 調べた 20 検体中 10 例がインフルエンザ A 陽性（50%）であった. そのうち A 型と B 型共に陽性が 2 検体で, B 型のみ陽性が 1 検体あった. PCR 法では 27 検体中 14 検体（52%）がインフルエンザ A 陽性であり, 季節性インフルエンザ（A ソ連型（H1N1））が 1 例検出された. 症例 30 は剖検肺材料のインフルエンザウイルスのより詳細な性状を解析した[9].

2. RT-PCR 法によるインフルエンザウイルス遺伝子の検出

RT-PCR 法にて新型インフルエンザウイルス遺伝子の検出を行った. 対象として従来の A ソ連型（H1N1）, A 香港型（H3N2）及び B 型インフルエンザウイルスのプライマーを使用した（Table 1）. Fig. 1A, B にそれぞれ症例 10, 13 の結果を示す. 症例 10 のレーン 5, 7 にそれぞれパンデミックインフルエンザウイルス NA, M1 遺伝子産物（1411 塩基, 758 塩基）が検出された. 症例 13 でも M1 のバンドが検出された.

3. 分離された新型インフルエンザウイルスによる細胞変性効果（CPE）

症例 10 の検体を接種した MDCK 及び CaCo-2 細胞における CPE を Fig. 2C, D に示した. 共に 2 代目継代 4 日後の CPE である. MDCK 細胞においては細胞の円形化が見られたが, 破壊された細胞の浮遊像はほとんど見られなかった. 一方, CaCo-2 においては細胞の円形化とその集合および細胞の浮遊像が多数見られた. また分離されたウイルスに対して HA 試験を行ったところ, ウイルスを分離した症例 10, 13 ともに MDCK 細胞では 20HA 価/50μL の力価を示したが, CaCo-2 細胞では共に 80HA 価/50μL で 4 倍高い力価を示した.

4. 血清学的診断

ペア血清（急性期：1〜3 病日, 回復期：2〜3 週間）が採取できた 3 症例（症例 12, 23, 26）の HI 抗体価

Table 1 Primers for RT-PCR

Subtype		Designation	Direction	Sequence	Target gene	Ampli-con (bp)
A/H1N1/Russia	RT	YI-16		5'AGCAAAAGCAGGGGAAAATA3'		
	1st and 2nd PCR	YI-01	FW	5'GAGGGAGCAATTGAGTTCAG3'	HA	479
		YI-13	RV	5'CCAAAGCCTCTACTCAGTGC3'		
A/H3N2/Hong Kong	RT	04NH1		5'TGAAGTGACTAATGCTACTG3'		
	1st PCR	04NH1	FW	5'TGAAGTGACTAATGCTACTG3'		
		04NH2	RV	5'TTGTCCAATAGATGCTTATT3'	HA	280
	2nd PCR	04NH3	FW	5'GCAACTGTTACCCTTATGAT3'		
		04NH4	RV	5'CCCCCAAATGTACAATTTGT3'		
Pandemic A/H1N1/2009	RT	RT1		5'AGCAAAAGCAGGT3'		
		RT2		5'AGCGAAAGCAGGT3'		
		RT3		5'AGCAAAAGCAGGC3'		
		RT4		5'AGCGAAAGCAGGC3'		
		RT5		5'AGCAAAAGCAGGG3'		
		RT6		5'AGCGAAAGCAGGG3'		
	1st PCR	RT1-RT6 mixture	FW			
		NA/Rev	RV	5'HHACTTGTCAATDGTDAATG3'	NA	1,411
	2nd PCR	NA/FW	FW	5'ATGAATHCAAAHCADADDAT3'		
		NA/Rev	RV	5'HHACTTGTCAATDGTDAATG3'		
	1st PCR	RT1-RT6 mixture	FW			
		M1/Rev	RV	5'TCACTTGAAHCGHTGHATHTGC3'	M1	758
	2nd PCR	M1/FW	FW	5'ATGAGTCTTCTAACCGAGGT3'		
		M1/Rev	RV	5'TCACTTGAAHCGHTGHATHTGC3'		

Table 2 Summary of medical history and clinical investigation

Case	Days after the onset	Age (yr)	Sex	Rapid test	RT-PCR	HI titer		Medical history	Others (travel)
						Acute	convalescent		
1	10	NR	F	−	+ seasonal	NT	NT	pregnant, arthralgia	Las Vegas (USA)
2	NR	NR	NR	+ A, + B	−	NT	NT	influenza encephalopathy	
3	1	29	F	−	−	NT	NT	a slight fever, anthralgia	
4	16	20	M	−	−	NT	NT	39℃, neck swelling	
5	1	24	F	−	NT	NT	NT	39℃, gastroenterisis	
6	3	52	F	−	NT	NT	NT	39.6℃, anthralgia, malaise	
7	NR	NR	NR	−	−	NT	NT	neonate, 39℃	
8	1	24	M	−	−	NT	NT	36.9℃, headache	
9	1	NR	NR	+ B	−	NT	NT	36.9℃, headache	
10	NR	24	NR	+ A	+ pandemic	NT	NT	fever	Okinawa (Japan)
11	1	NR	NR	NT	NT	NT	NT	NR	
12	NR	20	NR	+ A	+ pandemic	<10	40	rhinorrhea, cough	Okinawa (Japan)
13	NR	NR	NR	+ A	+ pandemic	NT	NT	NR	
14	NR	NR	NR	NT	−	NT	NT	fever, liver dysfunction, unconsciousness	
15	NR	NR	F	NT	−	NT	NT	pregnant	
16	3	66	F	+ A	+ pandemic	NT	NT	39℃, respiratory disorder	
17	2	9	F	NT	+ pandemic	NT	NT	respiratory disorder	
18	2	11	M	NT	+ pandemic	NT	NT	fever, cough, vomiting	
19	NR	NR	M	+ A, + B	−	NT	NT	NR	
20	3	54	F	NT	+ pandemic	NT	NT	38℃, rhinorrhea, anorexia	
21	NR	5	M	NT	+ pandemic	NT	NT	asthma	
22	1	9	M	NT	−	NT	NT	myocarditis, cardiopulmonary arrest	
23	1	20	F	NT	+ pandemic	10	80	38.2℃, cough, vomiting	
24	1	31	M	+ A	−	NT	NT	fever	
25	1	24	F	+ A	−	NT	NT	NR	
26	2	49	M	NT	+ pandemic	20	80	38℃, rhinorrhea, anorexia	
27	5	9	F	+ A	+ pandemic	NT	NT	37℃	
28	NR	11	F	−	+ pandemic	NT	NT	41℃, respiratory failure	
29	3	NR	NR	−	−	NT	NT	cough	
30	27	56	NR	+ A	+ pandemic	NT	NT	fever, pneumoniae	

+ A: influenza virus A; + B: influenza virus B; NR: no record; NT: not test

Fig. 1 RT-PCR products from patient's samples. A) patient case 10 B) patient case 13 M: size marker. RT-PCR was performed with primers specific for A/H1N1/Russia (lanes 1 and 2), A/H3N2/Hong Kong (lanes 3 and 4) and pandemic A/H1N1/2009 (lanes 5 and 8). The expected sizes of NA and M1 genes of pandemic A/H1N1/2009 are 1411 bp and 758 bp, respectively. *NC: Negative Control. **non-specific band. Expected size of A/H1N1 Russia is 479 bp.
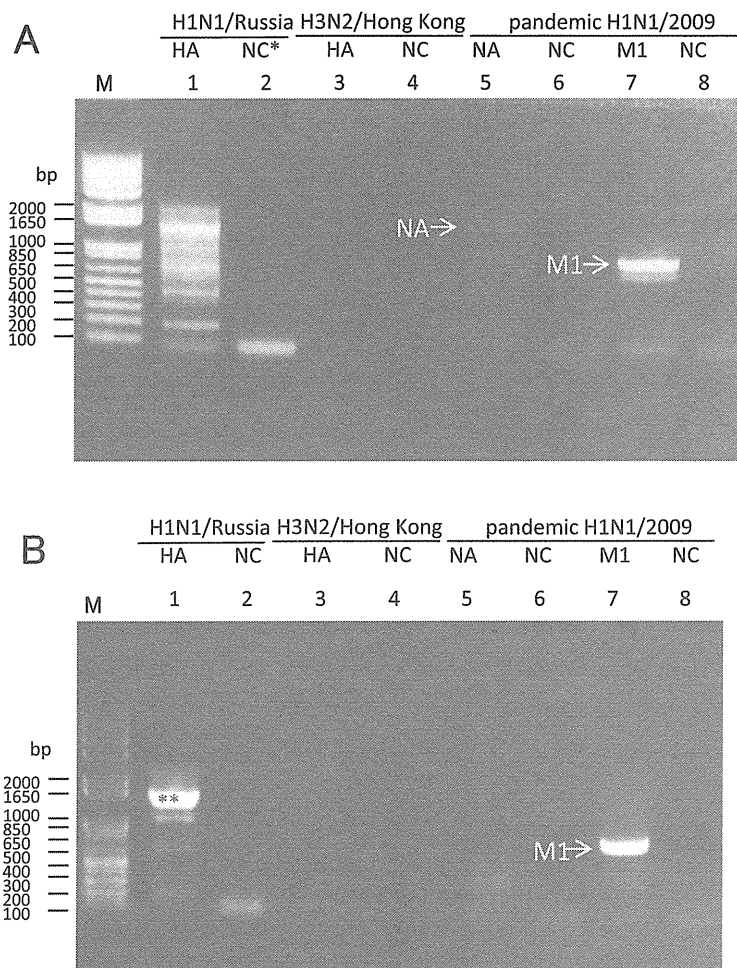
（Table 2）は急性期血清では10倍以下が1名，残りは10倍と20倍であった．一方，回復期血清では抗体価は40〜80倍となり，全て4倍以上の有意な抗体価の上昇がみられ，当該インフルエンザの感染が確認できた．

　5．成人の新型インフルエンザウイルスワクチン接種後の抗体価の変動

　Table 2に示した症例以外の成人健常者（24〜60歳）の新型インフルエンザウイルス抗体価を Table 3に示した．ワクチン接種前では11名中9名は10倍未満（82％）で，20倍（58歳男性）および40倍（41歳男性）がそれぞれ1名あった．一方，ワクチン接種後20日経過した後の抗体価は最大で640倍が1名で，40倍が6名で最も多く，80倍が3名であり，症例3, 10, 13を除いてすべて一般的に言われている感染防御レベル40倍以上の抗体価の上昇が見られた．

考　察

　今回の検査依頼症例の内訳は，新型インフルエンザという症候がまだ十分定まっていない状況も一因となって，発熱や筋肉痛などの典型的なインフルエンザ症状の症例に加え，多臓器不全例や剖検例（症例16及び30），脳症（症例14），心筋炎（症例23）などの重症例がある一方，学校や職場での感染防御上の必要性から鼻汁のみを軽く認める症例など多彩であった．この軽い症例の中にはパンデミック初期に当該インフルエンザ発生報告があった米国からの帰国や沖縄への旅行をしたものが含まれていた．将来起こることが予想される真の深刻なパンデミックの場合も同様な内訳が予想されるが，特に今回実施した通常の一般検査では依頼のない軽症者の当該施設による検査が潜在的感

平成25年5月20日

Fig. 2　Cytopathic effect (CPE) of pandemic influenza A (H1N1) 2009 4 days post inoculation. A: MDCK cells of mock inoculated; B: CaCo-2 cells of mock inoculated; C: MDCK cells inoculated with virus isolated from case 10; D: CaCo-2 cells inoculated with virus isolated from case 10.
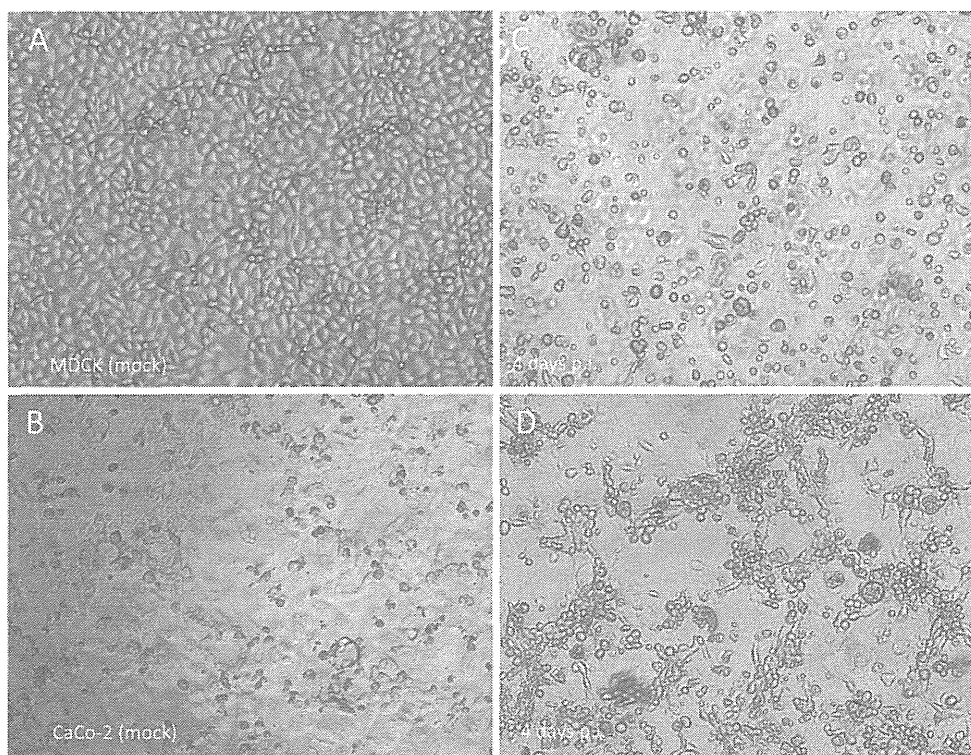

Table 3　Seroconversion by vaccination

| Case | Age | Sex | HI titer | |
			pre	post*
1	24	F	<10	80
2	34	F	<10	40
3	35	M	−	10
4	36	M	<10	40
5	37	M	<10	40
6	41	M	−	40
7	41	M	40	80
8	42	M	<10	80
9	48	F	<10	40
10	48	M	<10	20
11	51	M	<10	40
12	58	M	20	640
13	60	M	<10	20

*20 days after the vaccination

染者の把握とそれに続く感染防御策のため重要になると考える．したがって真のパンデミック時には機動力があり臨機応変な対応のできる当該類似施設が必須と考える．

　当初は，当該豚インフルエンザウイルスによるヒトの死亡例が大きくマスコミ等に取り上げられ社会不安が増大した．しかしCDCにより高齢者は力価は低い

がある程度の抗体を持つものが多いという発表により沈静化した[4]．我々もすぐに抗体価を調査し，11名中2名（18%）（Table 3）が低値であるが抗体を保有していることを確認した．最終的に感染率は低年齢層で高く，高齢者では低かったことからCDCの発表は正しかったことが示された．しかし一部の研究者は，超高齢者以外は抗体を持たないという反論を示した[10]．情報が此の様に錯綜した場合の行動規範として自ら調べることが必要と思われる．1976年の米国フォート・ディックス事件での豚インフルエンザ流行時に，森らは独自に福岡県において血清抗体価を測定した[11]．当時米国で発生したにもかかわらず福岡県人のかなりの割合がこの豚インフルエンザウイルスに対する抗体を保有している事を明らかにした．インフルエンザウイルスのような豚，鳥などが介在して伝播する病原体はヒトもすでに感染し，部分的にせよ抗体を獲得している場合があると考えられる．真の意味での新型インフルエンザアウトブレイクはないのではないかと考えられる．

　従来のインフルエンザウイルスワクチン（A/H1N1）2回接種後は通常HI価が40倍を超えるものが約90%以上見られる[12]．今回，新型インフルエンザワクチンでは11名中10名がHI価40倍以上（91%）に

上昇していた．その中には80倍（3名）または640倍（1名）にまで上昇した者もいた．つまり従来のワクチン2回接種とほぼ同様な反応であり，このことからも毎年感染することによる免疫のブースト効果が従来のソ連型インフルエンザウイルス並に存在したことがわかる．

なおウイルス分離に用いたCaCo-2細胞はウイルス力価がMDCK細胞を用いた場合の4倍有り，HI試験実施に際して有用であった．またCaCo-2細胞はインフルエンザウイルスやエンテロウイルスの分離率も高いという報告もあり[13]，今後のパンデミック時にはウイルス分離に優先的に使ってみる価値があると考えられる．

パンデミックにおいて独自の検査体制を構築し，抗原検査やPCR検査さらに抗体価測定などを積極的に行うことで，行政やマスコミさらにインターネットに流れる膨大な情報に惑わされることなく地域に密着した医療ならびに感染防御政策が実施できると考える．

文　献

1) CDC：Swine Influenza A (H1N1) Infections in Two Children—Southern California, March—April 2009. 2009；58：826—9.

2) 堺　春美，木村三生夫：どうなる今冬のインフルエンザワクチン WHO によるパンデミック宣言の真相解明のために欧州会議が調査を開始．臨床とウイルス　2010；38：1—54.

3) 加藤茂孝：人類と感染症との闘い—「得体の知れないものへの怯え」から「知れて安心」へ—第9回「インフルエンザ」—人類に最後まで残る厄介な感染症．モダンメディア　2011；57：39—54.

4) Hancock K, Veguilla V, Lu X, Zhong W, Butler EN, Sun H, et al.：Cross-reactive antibody responses to the 2009 pandemic H1N1 influenza virus. N Engl J Med 2009；361：1945—52.

5) 新型インフルエンザ対策ワーキンググループ：社団法人日本感染症学会緊急提言「一般医療機関に於ける新型インフルエンザの対応について」．2009-5-21 http://www.kansensho.or.jp/influenza/090522soiv_teigen.html.（参照5月）.

6) Faix DJ, Sherman SS, Waterman SH：Rapid-test sensitivity for novel swine-origin influenza A (H1N1) virus in humans. N Engl J Med 2009；361：728—9.

7) 泉　信有：インフルエンザ診断における簡易キットの役割．日医雑誌　2010；139：1486.

8) Tai CF, Lu CY, Shao PL, Lee PI, Chang LY, Huang LM：Rapid-test sensitivity for novel swine-origin pandemic influenza A. J Formos Med Assoc 2012；111：427—30.

9) Hamada N, Imamura Y, Hara K, Kashiwagi T, Nakazono Y, Chijiwa K, et al.：Intrahost emergent dynamics of oseltamivir-resistant virus of pandemic influenza A (H1N1) 2009 in a fatally immunocompromised patient. J Infect Chemother 2012；18：865—71.

10) Itoh Y, Shinya K, Kiso M, Watanabe T, Sakoda Y, Hatta M, et al.：In vitro and in vivo characterization of new swine-origin H1N1 influenza viruses. Nature 2009；460：1021—5.

11) 福吉成典，武原雄平，杉島伸禄，森　良一，小田　鉱：ブタインフルエンザウイルスA/NJ/9/76に対する抗体保有調査．福岡医学雑誌　1976；67：301—3.

12) 三上稔之，筒井理華，佐藤　孝，大友良光，木村三生夫，鈴木　功，他：介護老人保健施設におけるインフルエンザワクチン接種成績について（1998～1999）．臨床とウイルス　2000；28：219—36.

13) 吉野修司，山本正悟，川畑紀彦：Caco-2細胞を用いたインフルエンザウイルスの分離．感染症誌　1998；72：347—51.

平成25年5月20日

Review of a Community-based Laboratory Diagnosis of Pandemic Influenza A (H1N1) 2009

Yoshihiro IMAMURA, Nobuyuki HAMADA, Koyu HARA, Takahito KASHIWAGI & Hiroshi WATANABE
Division of Infectious Diseases, Department of Infectious Medicine, Kurume University School of Medicine

We performed a community-based laboratory diagnosis of pandemic influenza A (H1N1) 2009 with the RT-PCR technique using originally constructed primers. Of 30 patients who were suspected to be infected with the influenza virus from May 2009 until January 2010, the A (H1N1) 2009 virus was detected in 13 patients (43.3%). Three cases were immunologically confirmed to be infected with the A (H1N1) 2009 virus, because significant increases in the HI titer were observed in the convalescent sera. We also measured the antibody titers to the A (H1N1) 2009 virus in 13 healthy individuals with the HI assay using originally isolated virus. In most cases, the HI antibody titers were less than 10, except two cases with titers of 40 and 20. Our inspection system organized in the early phase of the A (H1N1) 2009 pandemic contributed to disease control in an outpatient clinic and a hospital in a small city. The process which we used to construct the system would be a good reference for a treatment protocol in the case of a future literal pandemic.

特集／グローバル化する感染症の最新情報

渡 航 前 に 予 防 す べ き 疾 患 と 接 種 す べ き ワ ク チ ン

日 高 秀 信　　　渡 邊　　浩

　近年，邦人の海外渡航者は増加の一途をた
どっており2012年度の渡航者数は1,800万人を
超えた。開発途上国ではさまざまな感染症に罹
患するリスクが高くなるため，渡航前に十分な
準備が必要である。感染症は，ワクチンで予防
できる疾患とワクチンでは予防できない疾患に
大別されるが，国や地域によって流行状況が異
なるため，接種が必要なワクチンも異なる。日
本医師会では，表1のように渡航地域ごとに推
奨ワクチンを大まかに提示しているが，実際の
渡航外来ではこのほかCDCのウェブサイト[1]，
厚生労働省検疫所ウェブサイト（FORTH）[2]な
どの公的情報源やTropimed®などの市販の有
料ソフトなどをもとにより詳しく個々の状況に
応じた対応が必要となる。以下に渡航時に予防
すべき疾患と必要となるワクチンを紹介する。

I. 渡航時に予防が必要な疾患のうちワクチンで予防可能な疾患

1. A 型 肝 炎

　汚染された食べ物や飲み物などを介して感染
する。潜伏期間2～6週間ののち，発熱，食欲
不振，倦怠感などが見られ，黄疸を呈する。劇
症化の頻度は，0.1～0.3％とされており，慢性
化することはなく一般的には予後良好な疾患で
あるが1ヵ月程度の療養が必要となることが多
い。予防は流行地における手指衛生，水や食べ
物への配慮（非加熱および加熱不十分な食べ物
を避け，飲用には飲料用の水を購入して飲むな
どの対応が必要。生野菜，カットフルーツ，氷
などもリスクが高い。）など一般的な経口感染

表　1　　　海外旅行必携ハンドブック2007日本医師会[3]より抜粋

ワクチン名	北 米	中南米	東アジア	南アジア	中近東	アフリカ	欧 州
ポ リ オ	×	×	△	○	△	△	×
ジフテリア	×	×	×	×	×	×	△
破 傷 風	○	○	○	○	○	○	○
日 本 脳 炎	×	×	○	○	×	×	×
A 型 肝 炎	×	○	○	○	○	○	×
B 型 肝 炎※	△	○	○	○	○	○	△
狂 犬 病	△	△	△	△	△	△	△
黄 熱	×	○	×	×	×	○	×
コ レ ラ	×	×	×	×	×	×	×
チ フ ス	×	×	○	○	△	△	×
ペ ス ト	△	△	△	×	×	△	×

久留米大学医学部感染医学講座臨床感染医学部門